Fugacity Coefficients for Free Radicals in Dense Fluids: HO_2 in Supercritical Water

Tahmid I. Mizan, Phillip E. Savage, and Robert M. Ziff
Dept. of Chemical Engineering, University of Michigan, Ann Arbor, MI 48109

The fugacity coefficients of the hydroperoxyl radical in supercritical water are estimated through molecular simulations. A potential function for the radical is first derived from ab initio self-consistent field molecular orbital calculations at the unrestricted Hartree-Fock level and from data in the literature. Molecular dynamics simulations of the hydroperoxyl radical are then performed in supercritical water and the fugacity coefficient of the radical is calculated by the free-energy perturbation method using the dynamic coupling parameter window-modification technique. The values of the fugacity coefficients at 773 K differ from unity. This methodology facilitates the incorporation of thermodynamic nonidealities in mechanism-based kinetic models for free-radical reactions in supercritical water.

Introduction

Water at elevated temperatures and pressures is attracting interest as a reaction medium and an environmentally benign alternative to organic solvents (Savage et al., 1995; Parsons, 1996; Sealock et al., 1993; Siskin and Katritzky, 1991). Several of the reactions investigated in near- or supercritical water (SCW) are governed by free-radical chemistry. Among these reactions the complete oxidation of (hazardous) organic compounds in supercritical water is a noteworthy example.

Rigorous kinetic models for free-radical reactions in supercritical water require thermodynamically consistent rate constants for the forward and reverse directions of each elementary reaction step. This means the reverse rate constant, k_r, must be calculated from the forward rate constant, k_f, and the concentration-based equilibrium constant, K_c. This constant is obtained from the activity-based equilibrium constant, K_a, and the fugacity coefficient correction, K_ϕ

$$\frac{k_f}{k_r} = K_c = \frac{K_a}{K_\phi}\left(\frac{P_0}{ZRT}\right)^{\Sigma \nu_j}, \tag{1}$$

where

$$K_\phi = \prod_j \phi_j^{\nu_j}. \tag{2}$$

Equation 1 shows that for thermodynamically nonideal fluid phases, such as supercritical water, fugacity coefficients for each of the reacting species, radicals included, are required to ensure thermodynamically consistent rate constants. For stable molecules, for which the critical properties and acentric factor are known, the fugacity coefficients can be calculated from an equation of state. On the other hand, there is currently no method for obtaining reliable estimates of fugacity coefficients for free radicals in a dense medium, yet these values have a strong influence on the results generated by mechanistic kinetics models (Schmitt and Butler, 1995). This article describes the first such method, which uses computational quantum chemistry and molecular dynamics (MD) simulations, and then illustrates the application of this method by considering the hydroperoxyl radical (HO_2) in supercritical water at 773 K.

Free energies of solutes in aqueous or supercritical solutions

Well-established methods exist for calculating the free-energy difference between two states or species from molecular simulations (e.g., Hummer and Szabo, 1996), and these methods have been used previously to calculate activity coefficients, residual chemical potentials, and solvation free energies for solutes in aqueous or supercritical solutions. For example, Haile (1986) reviewed the use of the Kirkwood coupling parameter for determining activity coefficients and other

Correspondence concerning this article should be addressed to P. E. Savage.
Present address of T. I. Mizan: Department of Chemical Engineering, University of Delaware, Newark, DE 19716.

thermodynamic measures from molecular simulations. He calculated the excess Gibbs free energy of 14 repulsive soft-sphere mixtures and found that the simulations yielded values that agreed with thermodynamic perturbation theory to within 5%. Shing and Chung (1987) expounded a method based on the Kirkwood formalism for determining the residual chemical potential from molecular simulations. They applied this method to a supercritical carbon dioxide–napthalene system represented by Lennard-Jones spheres plus quadrupole interactions. They used their results to estimate solubilities as a function of pressure and found qualitative agreement with experiment. Lazaridis and Paulaitis (1993) determined the ratios of activity coefficients for a large number of organic solutes in water at ambient conditions using Monte Carlo simulations. Recently Balbuena et al. (1996) estimated the free energies of solvation of a number of ionic and molecular species in water at ambient and supercritical conditions.

All of these previous molecular simulation studies of solutes or supercritical solutions considered species for which intermolecular potential models were available in the literature. Moreover, none of these previous studies considered free radicals, which are the solutes of interest in the present investigation. The literature provides potential models for a few small alkyl radicals (Liu and Allinger, 1994), but no model is available for HO_2, the radical of interest in this study. Consequently, a large portion of the work reported herein was devoted to establishing a reasonable potential model for HO_2. The next subsection explains our motivation for selecting HO_2 in supercritical water as the system to study.

Hydroperoxyl radical in supercritical water

Supercritical water is a promising and environmentally innocuous medium for chemical processes because many of its properties can be tuned by adjusting the temperature or pressure, it is completely miscible with organic compounds and permanent gases, and it is nontoxic. Among the various reaction processes being envisioned in SCW, supercritical water oxidation (SCWO) is perhaps the most established, as evidenced by the commissioning of a commercial SCWO reactor (Parkhill, 1995).

The hydroperoxyl radical plays a key role in SCWO reactions. Brock et al. (1996), Brock and Savage (1995), Gopalan and Savage (1995), and Holgate and Tester (1993, 1994) have all found that HO_2 is an important intermediate for methane, methanol, carbon monoxide, and hydrogen oxidation in SCW. For example, Brock and Savage (1995) showed that of the 148 elementary free-radical reactions included in their mechanism, fewer than 20 played a dominant role in the oxidation kinetics and nearly half of these dominant reactions involved HO_2. Likewise, Gopalan and Savage (1995) demonstrated that of the 123 elementary reactions involving 62 species in their reaction mechanism for the oxidation of phenol in SCW, four of the nine reactions to which phenol conversion was most sensitive contained the hydroperoxyl radical. Clearly, the hydroperoxyl radical is a species of major importance in oxidation kinetics in supercritical water.

These efforts to model the oxidation chemistry and kinetics by means of a large number of elementary reactions are aimed at aiding the rational design of SCWO processes and reactors. The lack of reliable methods to calculate the fugacity coefficients for free radicals required for these models has led to two different approaches for implementing these models. The most common approach has been to use the ideal-gas assumption wherein K_ϕ is set to unity. Indeed, existing mechanistic models using ideal-gas thermodynamics adequately describe SCWO at high temperatures (which approximate ideal gas conditions), indicating that the chemistry involved is essentially captured by these models. At lower temperatures, however, where conditions in SCW are much different from an ideal gas, K_ϕ should not be set to unity. The second approach is to treat SCW as a real gas and determine K_ϕ for elementary reactions involving free radicals by estimating values for the critical properties of the radicals involved using group contribution techniques (Reid et al., 1988). This approach has been used in the Real Gas modification of the CHEMKIN software package (Schmitt et al., 1994). The values of the fugacity coefficients obtained by such estimates of the critical properties are highly uncertain.

In this study, we obtain more reasonable estimates of fugacity coefficients of free radicals through molecular simulations. As a test case we take up the system of the hydroperoxyl radical in supercritical water. Our method consists of two steps, first we establish potential functions for the free radical and the solvent molecule. We then calculate the solvation free energy of the radical in the solvent and use this quantity to estimate the fugactiy coefficient. The following section describes how we devised a potential function for the hydroperoxyl radical. We then describe the molecular dynamics simulation methods used in this study. We discuss the calculation of solvation free energy through the perturbation technique and show how this free energy is related to the fugacity coefficient. The results of our simulations are then presented and discussed. Finally, we summarize the main conclusions of this work.

Potential Models

To perform molecular dynamics simulations one must first know the potential function describing the inter- and intramolecular interactions of the species in the system. A typical interaction potential function consisting of inter- and intramolecular terms is

$$U = \sum_{l=1}^{N-1}\left(\sum_{m=l+1}^{N}\sum_{i,j}\left\{4\epsilon_{iljm}\left[\left(\frac{\sigma_{iljm}}{r_{iljm}}\right)^{12}-\left(\frac{\sigma_{iljm}}{r_{iljm}}\right)^{6}\right]+\frac{q_{il}q_{jm}}{r_{iljm}}\right\}\right)+\sum_{l=1}^{N}\left(\sum_{\text{all bonds}}\frac{1}{2}k_b(r-r_0)^2+\sum_{\text{all angles}}\frac{1}{2}k_\theta(\theta-\theta_0)^2\right). \quad (3)$$

The intermolecular part consists of the Lennard-Jones term (the first term) and the Coulombic interaction term (the second term). The last two terms represent the (intramolecular) bond stretching and bond-angle bending modes.

We conducted separate sets of simulations for rigid and flexible versions of water molecules and the hydroperoxyl

radical. We recently reported (Mizan et al., 1996b) on the effect of flexibility for simulations of supercritical water, and using both rigid and flexible models in this study provides an extension of these earlier comparisons. The rigid molecules have no intramolecular degree of freedom, so the last two terms of Eq. 3 are absent. We used the Lorentz-Berthelot combining rules for nonbonded (Lennard-Jones) interactions between dissimilar atom types. The potential functions used for water and the hydroperoxyl radical are described below.

Water

The rigid water model employed in these simulations is the simple point charge (SPC) model potential of Berendsen et al. (1981). The SPC water model is characterized by a charge located at each of the three atoms and a Lennard-Jones interaction potential centered on the oxygen atom. The values of the Lennard-Jones parameters and charges of the SPC model are given by Berendsen et al. (1981).

The flexible molecule simulations employed a flexible version of the SPC model proposed by Teleman et al. (1987), which we will refer as the TJE (Teleman, Jönsson, Engström) model. The intermolecular part of the TJE potential is identical to the SPC model, but it has an additional intramolecular part consisting of simple harmonic terms corresponding to the bending and stretching modes of the water molecule. The numerical values of the potential parameters of the TJE model are given by Teleman et al. (1987).

In previous work we have reported various thermodynamic, structural, transport, and dielectric properties of pure SCW using the TJE model (Mizan et al., 1994, 1997), compared these properties to those of the SPC model (Mizan et al. 1996b), and also examined hydrogen bonding in SCW using the TJE model (Mizan et al., 1995, 1996a).

Hydroperoxyl radical

The literature provides no potential model for the hydroperoxyl radical, so a large part of our effort was directed toward using computational quantum chemistry along with spectroscopic data in the literature for this radical to develop a potential model. Lubic et al. (1984) reported the equilibrium geometry of the hydroperoxyl radical in the ground state ($^2A''$), and Table 1 displays the bond lengths and bond angle. Both the OH bond length and the bond angle for this radical are comparable to those of water; however, the OO bond is considerably longer than the equilibrium OH bond found in water. The discussion below explains the development of each element in the potential function of this radical.

Intramolecular Potential Parameters. Uehara et al. (1985) reported spectroscopic data that provide the harmonic force constants for the bond-stretching and bond-angle bending terms for HO_2. Table 1 displays these force constant values. The bond-angle force constant is larger than the values used for the TJE model of water, whereas both of the bond-stretch force constants are smaller than the bond-stretch force constant of the TJE model. Although data for crossterms are available, we excluded these terms in the HO_2 model for the sake of simplicity and to be consistent with the flexible TJE model (which has no crossterms) used to represent water.

Lennard-Jones Parameters. Table 1 also provides the Lennard-Jones parameter values used for HO_2. The oxygen atom nearer to the hydrogen is labeled O1, and the distant oxygen atom is labeled O2. This nomenclature is used throughout this work. The Lennard-Jones parameters suggested by Weiner et al. (1986) for a hydroxylic oxygen were used for the two oxygen atoms, whereas parameters for the hydrogen atom were determined by adjusting the values Weiner et al. (1986) suggested for hydroxylic hydrogen to obtain a minimum energy HO_2-water dimer that agreed with the quantum mechanically (QM) calculated dimer described later.

Table 1. Parameters for the Hydroperoxyl Radical

Parameters		Reference
r_{OO}, Å	1.33	Lubic et al., 1984
r_{OH}, Å	0.97	Lubic et al., 1984
θ_{HOO}	104.3°	Lubic et al., 1984
k_{OO}, kJ/mol·Å^2	3,539	Uehara et al., 1985
k_{OH}, kJ/mol·Å^2	4,019	Uehara et al., 1985
k_{HOO}, kJ/mol·rad^2	581	Uehara et al., 1985
σ_H, Å	1.39	
σ_{O1}, Å	2.94	Weiner et al., 1986
σ_{O2}, Å	2.94	Weiner et al., 1986
ϵ_H, K	6.0	
ϵ_{O1}, K	75.5	Weiner et al., 1986
ϵ_{O2}, K	75.5	Weiner et al., 1986
q_H, e	0.419	
q_{O1}, e	−0.358	
q_{O2}, e	−0.061	

Partial Charges. We estimated net atomic partial charges for the hydroperoxyl radical by fitting the partial-charge-based electrostatic potential to the quantum mechanical electrostatic potential obtained from *ab initio* self-consistent field molecular orbital (SCF-MO) calculations at the unrestricted Hartree-Fock (UHF) level.

Although the net atomic charge is not an exact quantum mechanically defined property, it is nonetheless a very useful quantity. Net atomic charges are a computationally efficient way of approximating the electrostatic interactions between molecules in molecular dynamics simulations. Moreover, net atomic charges have been used as an indicator of the reactivity of a particular atomic site (Cox and Williams, 1981).

The quantum mechanical electrostatic potential (ESP) for a unit positive charge at a point $\boldsymbol{r}$ is defined as

$$V^{QM}(\boldsymbol{r}) = \sum_A \frac{Z_A}{|\boldsymbol{r} - \boldsymbol{R}_A|} - \sum_{mn} P_{mn} \int \frac{\phi_m \phi_n}{|\boldsymbol{r} - \boldsymbol{r}'|} d\boldsymbol{r}' \qquad (4)$$

where the first term represents the nuclear contribution, $\boldsymbol{R}_A$ is the position of nucleus A and Z_A is its charge, P_{mn} is the density matrix element of the wavefunction, and ϕ_m refers to the atomic basis function. The quantum mechanical ESP was calculated at about 4,000 Cartesian grid points around HO_2 using the GAUSSIAN90 (Frisch et al., 1990) package. The grid points were generated using our modification of the CHELPG program of Breneman and Wiberg (1990). A grid spacing of 0.3 Å was used in all calculations (except where otherwise mentioned). Grid points extended to a maximum radius of 2.8 Å from the nuclei. Points within the van der Waals (VDW) radii of the nuclei (1.45 Å for the hydrogen

nucleus and 1.7 Å for the oxygen nuclei) were excluded from consideration.

The array of quantum mechanically derived ESP values was then fit to atom-centered partial charges by a Lagrangian multiplier least-squares fitting technique, again using our adaptation of the CHELPG code (Breneman and Wiberg, 1990). During the fitting process the total molecular charge was constrained to fit the exact value of zero. The molecular dipole moment was not constrained.

The atom-centered ESP-derived charges calculated from the procedure described above for the HO_2 radical in its experimental equilibrium geometry (Uehara et al., 1985) are given in Table 2 for different levels of theory (different basis sets). For completeness, Table 2 also provides the Mulliken (1955) charges, which are part of the standard GAUSSIAN90 output. It is evident from Table 2 that the charges calculated from the Mulliken method do not vary in a systematic manner from one level of theory to another, whereas the ESP-derived charges clearly tend to converge to a set of values as higher levels of theory (larger basis sets) are invoked. Table 2 also gives the $\langle s^2 \rangle$ values calculated for the different levels of theory. These expectation values of the s^2 operator are all close to 0.75, which confirms that we indeed have the doublet (pure spin) state of the hydroperoxyl radical.

How well the set of partial charges mimics the quantum mechanical ESP, V^{QM}, may be ascertained by comparing the contour maps of the quantum mechanical ESP with the ESP produced by the three partial charges, $V^{ESP\text{-}fit}$. Figure 1a and 1b clearly demonstrate that the three atom-centered charges reproduce V^{QM} both qualitatively and quantitatively to a reasonable degree. One shortcoming of $V^{ESP\text{-}fit}$ is, however, apparent. A region of slightly less negative potential in the potential trough found in V^{QM} to the right of the two oxygen atoms is not observed for $V^{ESP\text{-}fit}$. Thus, for V^{QM} there are two potential valleys in this region, whereas for $V^{ESP\text{-}fit}$ there is but a single large valley. This shortcoming must be viewed in the context of the difficulty associated with fitting the property of a complex wavefunction to just three parameters. The differences between V^{QM} and $V^{ESP\text{-}fit}$ are plotted in Figure 1c. The ridge between the two valleys in the contour plot for V^{QM} manifests itself in the difference plot as a region of positive potential. It is also clear from this plot that $V^{ESP\text{-}fit}$ underestimates the ESP around the distal oxygen, O2.

A numerical estimate of the mismatch between V^{QM} and $V^{ESP\text{-}fit}$ may be obtained from the root-mean-square (rms) deviation, σ, defined as

$$\sigma = \sqrt{\frac{\sum_i (V_i^{QM} - V_i^{ESP\text{-}fit})^2}{N}} \qquad (5)$$

where the subscript i refers to the ith grid point of a total of N grid points. The σ values for the HO_2 radical are less than 12 kJ/mol at all levels of theory. This numerical value may be understood in the context of the difference plot, Figure 1c, in which the difference values vary from 5 to 15 kJ/mol in the region surrounding the VDW spheres of the nuclei. Extreme values for V^{QM} and $V^{ESP\text{-}fit}$ at the peaks and valleys shown in Figure 1a and 1b are around 100 and -100 kJ/mol.

Although the σ values and the comparison of the quantum mechanical ESP to the partial-charge-based ESP are useful, they do not indicate how accurately the set of charges represents the ESP in the neighborhood of the real hydroperoxyl radical. An indication of the accuracy of the charges can, however, be obtained by comparing the dipole moment produced by the ESP-derived charge distribution to its experimental value (Saito and Matsumura, 1980). Figure 2 provides this comparison. It is clear that at the higher levels of theory the ESP-derived dipole moment, indicated on the figure by the open triangles, is essentially equal to the experimental dipole moment represented as a dashed line. The figure also shows that the ESP-derived dipole moment is largely independent of the basis set for any reasonably sized basis set. On the other hand, dipole moments calculated using Mulliken charges (filled circles) do not reproduce the experimental dipole moment accurately and are extremely basis set dependent. Our results suggest that the atom-centered charges derived at the UHF/6311+G(d,p) level give a reasonably accurate description of the electrostatic environment around the hydroperoxyl radical. We also calculated the atom-centered partial charges for HO_2 at a UHF/6311+G(d,p) level using a finer grid spacing of 0.2 Å, which resulted in about 13,000 grid points. This extra effort did not produce any change in the charges obtained or in the rms deviation.

Table 2. Atom-Centered Partial Charges for the Hydroperoxyl Radical with Experimental Equilibrium Geometry

		ESP-Fitted			Mulliken		
Level of Theory	$\langle s^2 \rangle$	q_H	q_{O1}	q_{O2}	q_H	q_{O1}	q_{O2}
UHF/STO −3G	0.755	0.315	−0.302	−0.013	0.211	−0.194	−0.017
UHF/631 +G(d)	0.762	0.424	−0.359	−0.065	0.503	−0.486	−0.017
UHF/631 +G(d,p)	0.762	0.422	−0.355	−0.067	0.381	−0.339	−0.042
UHF/6311 +G(d,p)	0.762	0.419	−0.358	−0.061	0.269	−0.214	−0.055

Minimum energy hydroperoxyl-water dimer

Having established separately potential functions for the hydroperoxyl radical and water we felt it would be prudent to investigate the combined hydroperoxyl-water potential to ensure that the mixed system behaves in a reasonable manner. Unfortunately, there is no experimental information with which to validate the combined potential model. As an alternative we decided that careful quantum mechanical calculations would provide an acceptable surrogate to experimental data.

We examined hydroperoxyl-water dimers in which the monomers were internally rigid but were allowed to rotate and translate relative to each other to attain a minimum energy configuration. These geometry optimization calculations were also performed with GAUSSIAN90. The optimizations were initiated from different in-plane and out-of-plane geometries having various symmetries. Most of the starting configurations ended up as the optimized dimer shown in Figure 3, and this planar configuration was found to be the global minimum energy dimer. The geometry optimizations were performed at the unrestricted Hartree-Fock level with a 6-31+G(d,p) basis set (UHF/6-31+G(d,p)). Dimerization ener-

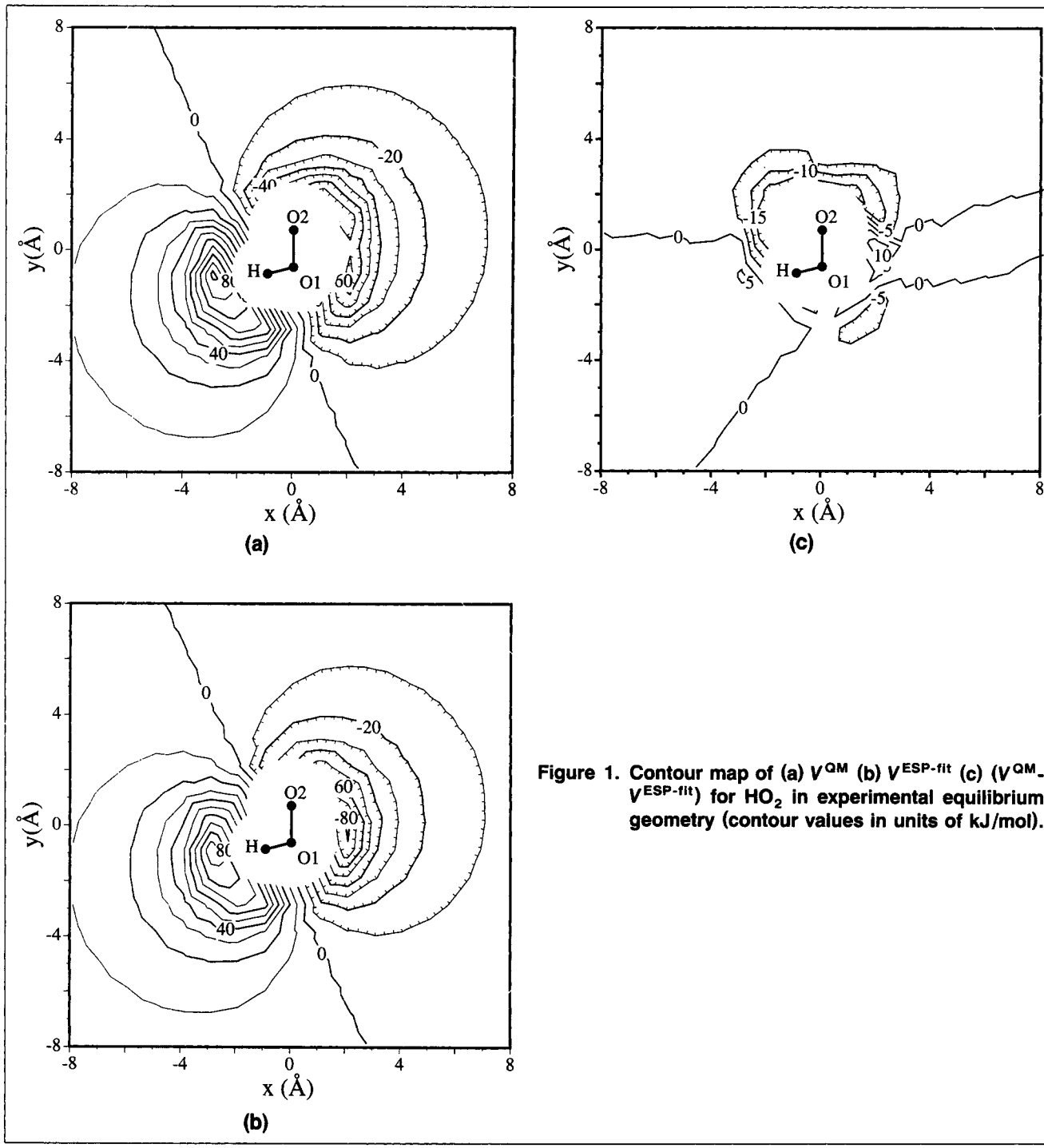

Figure 1. Contour map of (a) V^{QM} (b) $V^{ESP\text{-}fit}$ (c) (V^{QM}-$V^{ESP\text{-}fit}$) for HO_2 in experimental equilibrium geometry (contour values in units of kJ/mol).

gies were also calculated at this level. These energies were corrected for basis set superposition error (BSSE) by the counterpoise method of Boys and Bernardi (1970). Table 3 summarizes these energy calculations. Dimerization energies were also calculated at the second-order Møller-Plesset (Møller and Plesset, 1934) level (UMP2/6-31 + G(d,p) //UHF/6-31 + G(d,p)) with the geometry optimized at the unrestricted Hartree-Fock level. The Møller-Plesset calculations include electron correlation effects and are probably more accurate.

We compared the geometry and energies obtained from the quantum mechanical calculations described earlier to the geometry and energy obtained by minimizing our classical or molecular mechanical potential model dimer for the hydroperoxyl-water system. Table 4 provides this comparison. It is clear that both in terms of the separation between the radical and the water molecule and the inclination of the water molecule, the molecular mechanics results agree to within 3% of the quantum mechanical result. Extremely encouraging agreement is also obtained for the dimerization energy as cal-

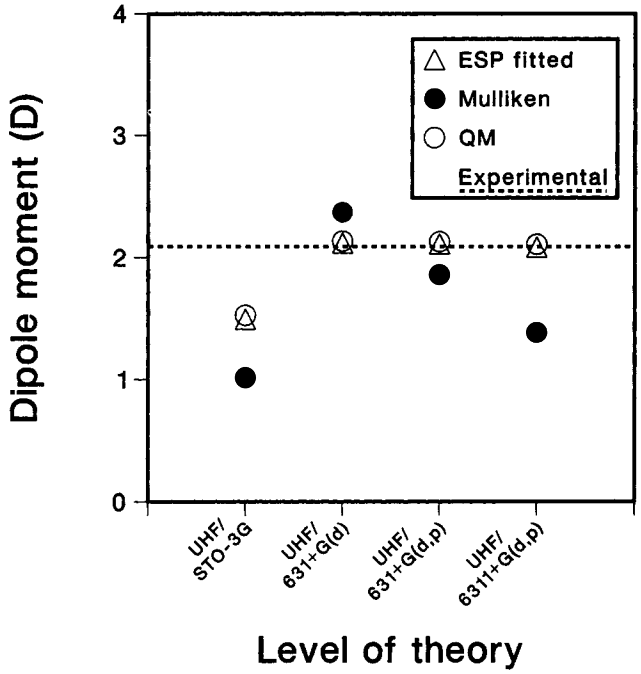

Figure 2. Dipole moments for atom-centered charges of HO_2 using experimental equilibrium geometry.

culated at the Møller-Plesset level and as calculated with our potential model.

In closing this section we note that there was also a very shallow minimum energy configuration, which is very similar to the configuration shown in Figure 3 except the positions of the water and HO_2 are interchanged. That is, one hydrogen atom of the water molecule was pointed toward the middle oxygen atom of the radical. This configuration was also planar, but the depth of this minimum was so small as to be on the order of the uncertainty in quantum chemical calculations. Indeed, the BSSE corrected dimerization energy for this configuration at the UMP2/6-31+G(d,p)//UHF/6-31+G(d,p) level was only -2.3 kJ/mol, whereas quantum mechanically calculated energies are generally thought to be correct to, at best, 4 kJ/mol (Pople et al., 1989). Given this large uncertainty, we did not feel it would be fruitful to investigate this weak local minimum any further.

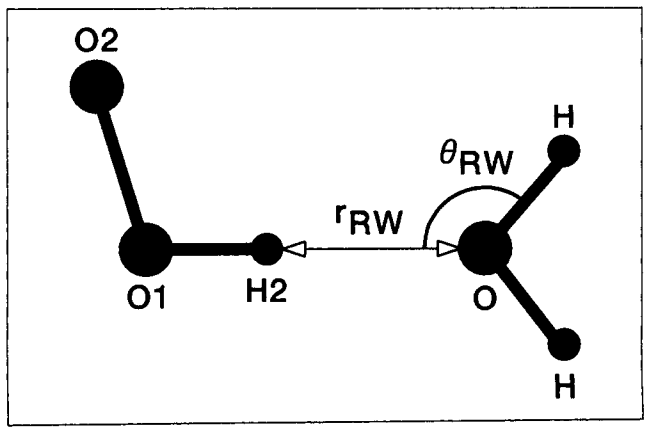

Figure 3. Minimum energy HO_2–H_2O dimer.

Table 3. Quantum Mechanical Energy of Dimerization of the Hydroperoxyl Radical with Water

Moiety	Level of Theory	Energy (hartree*)
HO_2+H_2O	UHF/6-31+G(d,p)	−226.22366224
HO_2+Bq**	UHF/6-31+G(d,p)	−150.18140363
H_2O+Bq	UHF/6-31+G(d,p)	−76.03165886
	Dimerization Energy	−0.01059974
HO_2+H_2O	UMP2/6−31+G(d,p) //UHF/6-31+G(d,p)	−226.7677873
HO_2+Bq	UMP2/6-31+G(d,p) //UHF/6-31+G(d,p)	−150.5209046
H_2O+Bq	UMP2/6-31+G(d,p) //UHF/6-31+G(d,p)	−76.2348556
	Dimerization Energy	−0.0120271

*1 hartree = 2,627 kJ/mol.
**One molecule of the dimer is made up of ghost atoms (Bq for *Banquo* in *Macbeth*) which have no nuclear charge but are provided with the appropriate basis functions

Calculation of Solvation Free Energy and Fugacity Coefficient

Perturbation technique for calculation of free energy

In this study we used the perturbation technique (Zwanzig, 1954) to calculate free energy through molecular dynamics simulations. This method is usually known as the free-energy perturbation (FEP) technique. The essence of this method is described below.

The Gibbs free-energy difference between any two states A and B is given by

$$\Delta G_{BA} = -k_B T \ln\left(\frac{\Delta_B(N,T,P)}{\Delta_A(N,T,P)}\right) = -k_B T \ln\left(\frac{\iint e^{-(H_B+PV)/k_BT}\,dV\,d\boldsymbol{p}^N\,d\boldsymbol{r}^N}{\iint e^{-(H_A+PV)/k_BT}\,dV\,d\boldsymbol{p}^N\,d\boldsymbol{r}^N}\right), \quad (6)$$

where Δ_B and Δ_A are the isothermal-isobaric partition functions. The second form of the equation shows these partition functions in the expanded form as integrals over volume and phase space of N momenta, $\boldsymbol{p}$, and positions, $\boldsymbol{r}$, with H_A to H_B being the Hamiltonians at the states A and B. If these states are very different, it is usually computationally expedient to the subdivide this free-energy difference across a number of narrower windows, N_w

$$\Delta G_{BA} = \sum_{i=1}^{N_w-1} \Delta G_{\lambda_i}, \quad (7)$$

Table 4. Geometry and Dimerization Energy of Minimum Energy Hydroperoxyl-Water

Level of Theory	r_{RW}, Å	θ_{RW}	Energy kJ/mol
UHF/6-31+G(d,p)	1.903	125°	−27.9
UMP2/6-31+G(d,p) //UHF/6-31+G(d,p)	1.903	125°	−31.6
Molecular mechanics	1.906	122°	−33.4

where λ_i is the value of the coupling parameter λ at window i with the Hamiltonian, H, being a function of λ, which can vary from zero to unity, thereby allowing the Hamiltonian to change continuously from H_A to H_B. Then

$$\Delta G_{\lambda_i} = -k_B T \ln\left(\frac{\Delta_{\lambda_i+1}(N,T,P)}{\Delta_{\lambda_i}(N,T,P)}\right)$$
$$= -k_B T \ln\left(\frac{\iiint e^{-(H_{\lambda_{i+1}}+PV)/k_BT}\, dV\, dp^N\, dr^N}{\iiint e^{-(H_{\lambda_i}+PV)/k_BT}\, dV\, dp^N\, dr^N}\right)$$
$$= -k_B T \ln\left(\frac{\iiint e^{-\Delta H_{\lambda_i}/k_BT} e^{-(H_{\lambda_i}+PV)/k_BT}\, dV\, dp^N\, dr^N}{\iiint e^{-(H_{\lambda_i}+PV)/k_BT}\, dV\, dp^N\, dR^N}\right), \quad (8)$$

where ΔH_{λ_i} is the perturbation to the Hamiltonian

$$\Delta H_{\lambda_i} = H_{\lambda_{i+1}} - H_{\lambda_i}. \quad (9)$$

The last form of Eq. 8 can be represented as the negative exponential of the dimensionless perturbation to the Hamiltonian ensemble averaged with respect to the state at λ_i (Reynolds et al., 1992), so that

$$\Delta G_{BA} = \sum_{i=1}^{N_w-1} -k_B T \ln\langle e^{-\Delta H_{\lambda_i}/k_BT}\rangle_{\lambda_i}. \quad (10)$$

Dividing the free-energy difference into a number of windows as described before avoids the orthogonality problem, which occurs when the perturbed and unperturbed states are very different and for which the ensemble may not contain a sufficient number of states with low values of the perturbation to the Hamiltonian. In our simulations we perturb the Hamiltonian forward to λ_{i+1} and backward to λ_{i-1} and obtain the quantity ΔG_{λ_i} for both the backward and forward perturbations. This technique is known as double-wide sampling (Jorgensen and Ravimohan, 1985). The backward and forward Gibbs free-energy increments are summed separately. If sufficient sampling is carried out at each window, these two increments should be approximately equal in magnitude and opposite in sign. The mean of the absolute values of the sums provides an estimate of the magnitude of the free-energy change and the difference between the magnitudes of the sums is an indication of the adequacy of the sampling at each window.

Usually in molecular simulation (Monte Carlo and molecular dynamics) evaluations of free-energy difference, the momentum contribution to the perturbation to the Hamiltonian is negligible (Pearlman and Kollman, 1989) and the perturbation to the Hamiltonian can be replaced by the perturbation to the potential energy function

$$\Delta G_{BA} = \sum_{i=1}^{N_w-1} -k_B T \ln\langle e^{-\Delta U_{\lambda_i}(r^N)/k_BT}\rangle_{\lambda_i}. \quad (11)$$

We used this approximation in our calculations.

The potential energy function $U(r^N)$ is a function of the positions and orientations of the molecules nominally represented by r^N. The various elements of the potential energy function described by Eq. 3 can be made functions of the coupling parameter λ

$$q(\lambda) = (1-\lambda)q^A + \lambda q^B \quad (12)$$
$$\epsilon(\lambda) = (1-\lambda)\epsilon^A + \lambda\epsilon^B \quad (13)$$
$$\sigma(\lambda) = (1-\lambda)\sigma^A + \lambda\sigma^B \quad (14)$$
$$k_b(\lambda) = (1-\lambda)k_b^A + \lambda k_b^B \quad (15)$$
$$r_0(\lambda) = (1-\lambda)r_0^A + \lambda r_0^B \quad (16)$$
$$k_\theta(\lambda) = (1-\lambda)k_\theta^A + \lambda k_\theta^B \quad (17)$$
$$\theta_0(\lambda) = (1-\lambda)\theta_0^A + \lambda\theta_0^B \quad (18)$$

such that when λ is zero the initial condition A is recovered, and when λ is unity the final condition B occurs. We employed the coupling parameter technique described above in our work.

We used the dynamically modified windows technique of Pearlman and Kollman (1989) to determine the increment in λ from one window to the next. In this technique the size of the increment in λ is adjusted to achieve a predetermined increment in the free energy, ΔG_{λ_i}, and thus depends on the rate of change of the free energy as a function of λ. This method has convergence characteristics that are superior to the fixed-window method in which the size of the λ increment remains fixed throughout the simulation. At each window, we allowed the system to equilibrate for 100–200 steps and then collected data over 100–200 production steps.

FEP method for flexible molecules

Free-energy perturbation (FEP) calculations of molecules having intramolecular degrees of freedom, particularly those in which these degrees of freedom are represented by harmonic functions, are fairly difficult because of the inherent orthogonality of perturbed and reference harmonic functions. The standard method of treating flexible degrees of freedom is the static perturbation of geometry (SPG) approach. In this approach, the bond length (or angle) obtained from the unperturbed or reference structure is used with the perturbed structure value of the equilibrium bond length and force constant to calculate the perturbed structure potential energy. The difference between the perturbed structure potential energy, U_B, and the reference structure potential energy, U_A, is typically large and usually positive, so that the simulations have very poor convergence properties. To avoid this problem Severance and Jorgensen (1995) developed the Generalized Alteration of Structure and Parameters (GASP) method for FEP calculations with flexible molecules.

In the GASP method the atomic coordinates are expressed as a perturbation to a reference coordinate r_f

$$r = r_f + \Delta r. \quad (19)$$

This changes the variable of integration in the partition function from r to Δr, and the FEP equation assumes the form

$$\Delta G_{AB} = -k_B T \ln \langle e^{-(U_B(r_{f,B},\Delta r) - U_A(r_{f,A},\Delta r))/k_B T} \rangle_A, \quad (20)$$

where A and B are the unperturbed and perturbed states, respectively. In the GASP formulation, values of r_f are allowed to differ between molecular states A and B. Then for the perturbation of a harmonic bond function

$$\Delta U_{AB} = U_B(r_{f,B}, \Delta r) - U_A(r_{f,A}, \Delta r)$$
$$= k_{b,B}((r_{f,B} + \Delta r) - r_{0,B})^2 - k_{b,A}((r_{f,A} + \Delta r) - r_{0,A})^2, \quad (21)$$

where k_b and r_0 are the force constant and equilibrium bond length, respectively. If $r_{f,B}$ is set equal to $r_{f,A}$, the SPG method is recovered. If, on the other hand, $r_{f,B}$ and $r_{f,A}$ have distinct values, and in particular, r_f is set equal to r_0, then the GASP method will be obtained. Free-energy perturbation calculations using the GASP method are faster and have more reliable convergence characteristics than those using the SPG method. We employed the GASP method in our flexible molecule simulations.

Solvation free energy and fugacity coefficient

In this subsection we follow derivations by Ben-Naim (1987) and Shing and Chung (1987) to develop an expression for the fugacity coefficient. Consider the case for which the initial and final states, A and B, in Eq. 6 correspond to the condition that an extra solute molecule that was not present in the system initially is present in the final state. For such a case the free-energy change corresponds to the solvation free energy or the chemical potential or partial molar Gibbs free energy, $\overline{G}_s$, of the solute for that particular state condition (Ben-Naim, 1987; Shing and Chung, 1987)

$$\overline{G}_s = G(N_s + 1, N_w, T, P) - G(N_s, N_w, T, P)$$
$$= -k_B T \ln \left[\frac{\Delta(N_s + 1, N_w, T, P)}{\Delta(N_s, N_w, T, P)} \right]. \quad (22)$$

The isothermal-isobaric partition functions can be separated into components attributable to positions and orientations of the molecules, to internal contributions, and to the translational motions (Shing and Chung, 1987). Then a new partition function Δ' that excludes these last two components can be defined

$$\Delta(N_s, N_w, T, P) = \frac{Q_S^{N_s} Q_W^{N_w}}{N_s!\, N_w!\, \Lambda_S^{3N_s} \Lambda_W^{3N_w}}$$
$$\int_0^\infty e^{-PV/k_B T}\, dV \int_V e^{-U(r^N)/k_B T}\, dr^N$$
$$= \frac{Q_S^{N_s} Q_W^{N_w}}{N_S!\, N_W!\, \Lambda_S^{3N_s} \Lambda_W^{3N_w}} \Delta'(N_S, N_W, T, P), \quad (23)$$

where Q_S and Q_W represent the internal contributions such as vibration, nuclear spin, and electronic contributions, and Λ_S and Λ_W are the thermal de Broglie wavelengths of the solute and water, respectively. The term $U(r^N)$ is the configurational potential energy of the system, which is a function of the position and orientation of the molecules. Shing and Chung (1987) derived the relation below for the partial molar Gibbs free energy of the solute in terms of this modified partition function, Δ'

$$\overline{G}_S = -k_B T \ln$$
$$\times \left[\left(\frac{Q_s}{\Lambda_s^3 (N_s + 1)} \right) \left(\frac{\Delta'(N_S = 1, N_W, T, P, \lambda = 1)}{\Delta'(N_S + 1, N_W, T, P, \lambda = 0)} \right) \langle V \rangle \right] \quad (24)$$

where $\langle V \rangle$ is the average volume of the system. At $\lambda = 0$, the $(N_S + 1)$th solute molecule vanishes. Since the terms in the first parentheses together with the system volume constitute the partition function for the solute in an ideal-gas mixture, Eq. 24 can be further simplified to

$$\overline{G}_S - \overline{G}_S^{IG} = -k_B T \ln \left[\frac{\Delta'(N_S + 1, N_W, T, P, \lambda = 1)}{\Delta'(N_S + 1, N_W, T, P, \lambda = 0)} \right]$$
$$= \sum_{i=1}^{N_w - 1} -k_B T \ln \langle e^{-\Delta U_{\lambda_i}(r^N)/k_B T} \rangle_{\lambda_i}. \quad (25)$$

This quantity $(\overline{G}_S - \overline{G}_S^{IG})$ is related to the fugacity coefficient of the solute as (Sandler, 1989)

$$\phi_S = \exp \left[\frac{\overline{G}_S(T, P, x_S) - \overline{G}_S^{IG}(T, P, x_S)}{RT} \right], \quad (26)$$

where x_S is the mole fraction of the solute. In our simulations, rather than introducing a solute molecule into the system, we make an existing solute molecule (or free radical, in this case) disappear because this process is computationally more convenient to simulate. We then reverse the sign of the calculated Gibbs free energy to obtain the quantity $(\overline{G}_S - G_S^{IG})$ or ΔG_{solv} as it will be called in this study.

Molecular Dynamics Techniques

All simulations were carried in a cubic cell with periodic boundary conditions in an isothermal-isobaric (NPT) ensemble using standard molecular dynamics techniques (Allen and Tildesley, 1987). The weak coupling method of Berendsen et al. (1984) was used to maintain the temperature and pressure at around the desired values using temperature and pressure relaxation time constants of 0.2 ps and 1 ps, respectively. The cutoff was based on molecular center-of-mass distance, and it was as large as possible given the dimensions of the simulation cell. A molecular cutoff ensures neutrality of charge. An automatically updated molecular neighbor list was employed. Except where otherwise mentioned, long-range Coulomb interactions were treated using the reaction-field method, in which the external dielectric constant defining the reaction field, ϵ_{RF}, was chosen to be 80. No long-range correction was made for the Lennard-Jones term of the intermolecular potential. The simulation system consisted of 255 water molecules and one solute moiety. Thus, the system was a mixture of 0.004 mole fraction of solute in water. Since the lone

solute moiety never interacts with another solute, however, such a system may be considered to be infinitely dilute. Ideally, we would have liked to simulate a truly infinitely dilute system. This would require an infinite, or at least a very large number (greater than 10^4) of solvent molecules. Such simulations are at present impracticable using the computational facilities available to us.

For the flexible molecule simulations, the equations of motion were integrated using the reversible reference system propagator algorithm (r-RESPA) (Tuckerman et al., 1992). This multiple time-step method treats rapidly varying forces, such as those responsible for bond stretch, in the short time step, while considering the slowly varying forces at the long time-step intervals. The algorithm was implemented in Cartesian coordinates. We considered bond-stretching forces at each short time-step interval and all other forces, namely, bond-angle bending forces and nonbonded forces at every long time-step interval. The long time step was set at 2 fs (femtosecond) and the short timestep at 0.25 fs (except where otherwise mentioned).

The method used for the rigid molecule simulations was identical to that for the flexible water simulations except that the equations of motion were integrated using the RATTLE method (Andersen, 1983). A time step of 2 fs was used.

Simulation lengths for the runs ranged from 100 ps to 1,300 ps. The average simulation length was 567 ps. These simulation durations are shorter than the runs on the order of nanoseconds that are considered to be necessary for free-energy calculations in ambient water. This is, however, to be expected because at supercritical conditions the diffusivity of water is about two orders of magnitude greater than at ambient conditions (Mizan et al., 1994). Thus, the rearrangement of the water molecules around the solute is considerably faster for SCW after each perturbation of the solute. For this reason we were able to obtain well-converged free-energy values with relatively short runs.

Results

Before attempting free-energy calculations for the hydroperoxyl radical in SCW we validated the perturbation method free-energy calculation computer code by calculating the solvation free energy of neon at nominally infinite dilution in liquid TIP3P water (Jorgensen et al., 1983) at ambient conditions. We obtained a value of 10.4 ± 1.3 kJ/mol that compares favorably with the value of 10.5 ± 0.8 kJ/mol published by Pearlman and Kollman (1989).

We also verified that our method would indeed yield reasonable values of fugacity coefficients. We calculated the fugacity coefficients of krypton at 0.004 mol fraction in argon at a supercritical temperature of 230 K and at various pressures. We used the Lennard-Jones parameters used previously by Schoen and Hoheisel (1984). The results appear in Figure 4a and are compared with the fugacity coefficients calculated using the Peng-Robinson (PR) equation of state using the critical properties given by Reid et al. (1988). It is evident that the results of the MD simulations enjoy good agreement with the results from the equation of state. Figure 4b compares the average molar volumes of our simulation systems to those calculated from the Peng-Robinson equation of state. Again, the agreement is very good.

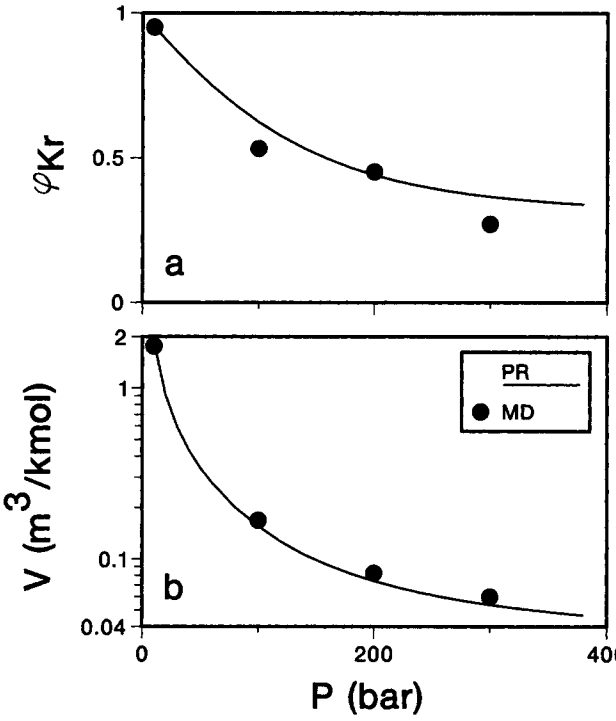

Figure 4. (a) Fugacity coefficients of Kr; (b) molar volumes in a Kr–Ar mixture at 230 K and various pressures.

Rigid-molecule simulations

We conducted several sets of molecular dynamics simulations at 773 K and at various pressures for the hydroperoxyl radical at nominally infinite dilution (0.004 mol fraction) in SCW. The hydroperoxyl radical was made to disappear, and the corresponding Gibbs free-energy change was calculated by the dynamic window perturbation method described earlier. The actual mutation of the radical to nothing was done in two stages by running two separate simulations for each set. In the first simulation, the atom-centered partial charges on the radical were reduced to zero, that is, the coupling parameter, which was changed from zero to unity, only affected the charges. In the second simulation, the Lennard-Jones parameters were reduced to zero, while at the same time all the bond lengths were reduced to 0.3 Å (the smallest bond length that will allow stable integration of the equations of motion). This separation of the different contributions is called electrostatic decoupling and has been recommended by Bash et al. (1987) as a way to achieve better convergence. Of course, free energy is a state property, so the free energy difference between the initial and final state is independent of the intervening conditions.

Figure 5a shows the free-energy change for the disappearance of charges from the HO_2 radical at 275 bar and 773 K. The final configuration for this simulation was used as the starting point for the next simulation in which the uncharged radical was made to vanish. The corresponding free-energy change is depicted as a function of the coupling parameter in Figure 5b.

As indicated previously one issue of concern in free energy calculations is the orthogonality of reference and perturbed

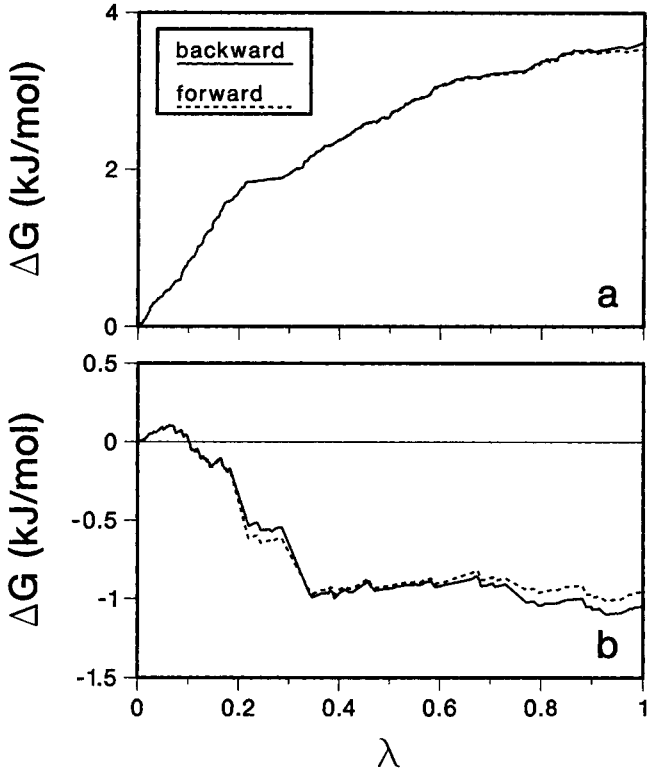

Figure 5. Free energy of desolvation for HO_2 in SCW at 773 K and 275 bar: (a) contribution from uncharging the radical; (b) contribution from disappearance of the uncharged radical.

states. This problem manifests itself in the jaggedness of the ΔG vs. λ trajectories. The problem is easily remedied (albeit at the expense of added computation time) by increasing the number of windows, that is, decreasing the coupling parameter increment. In our simulations we rejected ΔG vs. λ trajectories that appeared particularly jagged and repeated the run with a smaller λ increment. Another potential problem is sufficient sampling of the configurational space. This problem also becomes evident in the double-wide sampled ΔG vs. λ curves as a divergence between the forward and backward trajectories. Again, the problem is easily corrected by increasing the number of sampling steps. In our simulations, runs with diverging backward and forward trajectories were also repeated with an increased number of sampling steps.

ΔG_{solv} was calculated from several independent sets of simulations started from different initial configurations at each of four state conditions (275 bar, 775 bar, 1,500 bar, and 2,100 bar and 773 K). The mean, standard deviation and number of replicates for each state condition are reported in Table 5. The ΔG_{solv} values were then used to calculated the fugacity coefficients using Eq. 26.

Figure 6 shows the fugacity coefficients calculated for the rigid HO_2 in SCW modeled using the SPC potential. Our data points are depicted as crossed open squares. The dashed curve represents the fugacity coefficients of HO_2 in SCW calculated from the Peng-Robinson equation of state using the properties of HO_2 ($T_c = 400$ K, $P_c = 8.20$ MPa, $\omega = 0.200$) provided in the thermodynamic database supplied with the Real Gas version of CHEMKIN (Schmitt et al., 1994). The

Table 5. Free Energy of Solvation (kJ/mol) for Hydroperoxyl Radical in Supercritical Water at 773 K and 0.004 Mol Fraction

	Rigid		Flexible	
P, bar	No. of Runs	ΔG_{solv}	No. of Runs	ΔG_{solv}
275	4	-2.95 ± 0.45	3	-5.94 ± 1.57
775	3	-7.13 ± 0.97	1	-8.55 ± 0.26
1,500	2	-6.48 ± 0.81	1	-2.43 ± 0.78
2,100	3	-3.94 ± 2.51	2	0.19 ± 3.51

binary interaction parameters were set to zero. Clearly there is stark disagreement between our values and this curve. This lack of agreement need not be surprising when one considers that the critical properties given earlier for HO_2 are only rough estimates. Indeed, Schmitt et al. (1994) acknowledge that the uncertainty in these estimated critical properties is very large. That the fugacity coefficients from the MD simulations differ from those calculated from the Peng-Robinson equation with the estimated critical properties for HO_2 points out that the equation-of-state calculations for free radicals in the Real Gas version of CHEMKIN might not be reliable.

If we compare our data points in Figure 6 to the fugacity coefficient curve for pure SCW, generated using the Peng-Robinson equation of state with critical properties published in Reid et al. (1988), we observe that the values of the fugacity coefficients of HO_2 in SCW and pure SCW are very close in the range studied. This similarity, though interesting, is purely coincidental. The HO_2 data appear to go through a minimum between the 775-bar and 1,500-bar points, whereas the minimum for pure SCW occurs beyond the range depicted in the figure.

Sensitivity Analysis. In the absence of experimental thermodynamic data with which to validate our potential model for the HO_2-water system it is difficult to assess the accuracy

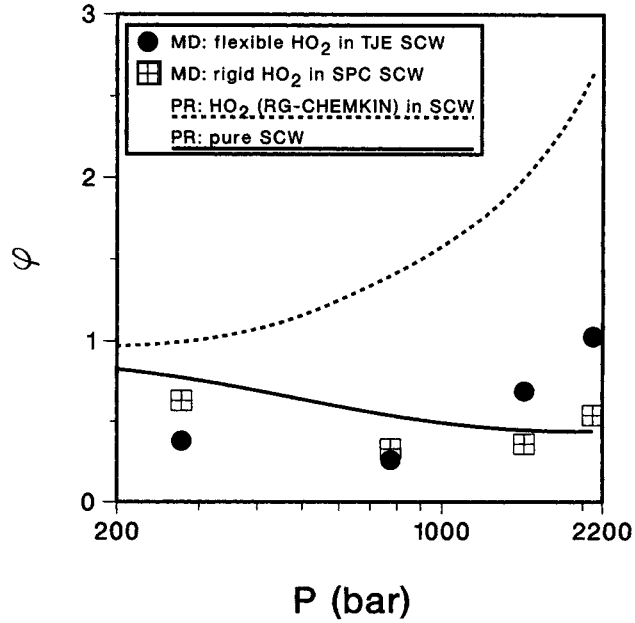

Figure 6. Fugacity coefficients for 0.004 mole fraction of solute at 773 K.

Table 6. Sensitivity Coefficients for Free Energy of Solvation of 0.004 mol fraction of rigid Hydroperoxyl Radical in SPC Supercritical Water at 773 K (in kJ/mol)

	P, bar			
	275	775	1,500	2,100
G	-2.95 ± 0.45	-7.13 ± 0.97	-6.48 ± 0.81	-3.94 ± 2.51
$\epsilon_H \partial G/\partial \epsilon_H$	0.16 ± 0.08	0.35 ± 0.04	0.39 ± 0.02	0.40 ± 0.01
$\epsilon_{O1} \partial G/\partial \epsilon_{O1}$	-0.06 ± 0.05	-0.24 ± 0.06	-0.48 ± 0.06	-0.55 ± 0.07
$\epsilon_{O2} \partial G/\partial \epsilon_{O2}$	-0.30 ± 0.02	-0.86 ± 0.08	-1.17 ± 0.04	-1.30 ± 0.07
$\sigma_H \partial G/\partial \sigma_H$	1.93 ± 0.73	4.30 ± 0.39	4.96 ± 0.16	5.32 ± 0.06
$\sigma_{O1} \partial G/\partial \sigma_{O1}$	6.55 ± 1.11	16.58 ± 1.03	21.29 ± 0.46	24.23 ± 0.90
$\sigma_{O2} \partial G/\partial \sigma_{O2}$	2.31 ± 0.21	6.12 ± 0.73	10.48 ± 0.73	12.08 ± 1.09
$q_H \partial G/\partial q_H$	-10.82 ± 3.85	-15.58 ± 1.35	-12.47 ± 0.41	-12.38 ± 0.72
$q_{O1} \partial G/\partial q_{O1}$	0.31 ± 1.61	-5.65 ± 0.47	-11.58 ± 0.40	-12.85 ± 0.75
$q_{O2} \partial G/\partial q_{O2}$	-0.50 ± 0.20	-1.93 ± 0.09	-3.07 ± 0.08	-3.31 ± 0.16

of the values of the fugacity coefficients previously reported. It is, however, possible to calculate how sensitive the free energies of solvation, and hence the fugacity coefficients, are to changes in the parameters of our potential model. Following Zhu and Wong (1993) we determined the free-energy sensitivity coefficients corresponding to the Lennard-Jones parameters and the partial charges. We did not examine the effect of varying the geometry or force constants because we use the experimental values of these quantities. We therefore limited our sensitivity analysis to the rigid molecule system.

The sensitivity coefficients reported in Table 6 were obtained from regular NPT molecular dynamics simulations (that is, simulations in which the solute was not made to vanish) of 50-ps duration. Four independent runs were conducted at each pressure. The means and standard deviations for each sensitivity coefficient are tabulated in the column under the corresponding simulation pressure. The first row of Table 6 gives the free energies of solvation taken from Table 5. These values can be compared with the sensitivity coefficients for each of the potential model parameters.

It is clear from Table 6 that at 275 bar, the free energy is most strongly influenced by the charge on the hydrogen atom. For instance, at 275 bar a 10% change in q_H would cause a 37% change in ΔG_{solv}, which in turn leads to a 20% change in the fugacity coefficient.

We believe that the uncertainty in the partial charge on the hydrogen atom is less than 10%. Recall that we verified the set of partial charges by comparing the calculated dipole moment, the electrostatic potential, and the geometry and energy of the minimum energy HO_2- water dimer to experimental and quantum mechanically derived values. We are therefore confident of the reasonableness of the set of charges. Thus, we can also be fairly confident of the free energy of solvation, and hence the fugacity coefficient calculated at low pressures.

Table 6 reveals that at the three higher pressures the largest sensitivity coefficient is the one for the Lennard-Jones σ parameter of the middle oxygen atom (O1). This parameter was taken directly from the force field of Weiner et al. (1986) and has been determined by fitting various physical properties of compounds containing a hydroxylic oxygen atom and is therefore considered to be a reasonable value.

To summarize, the calculated free energies are most sensitive to q_H and σ_{O1}. These parameters were carefully determined or taken directly from the literature, and we can expect their uncertainties to be fairly small.

Flexible-molecule simulations

Simulations involving flexible versions of the hydroperoxyl radical and water were also conducted at 773 K at the same average pressures as the rigid system. The GASP technique (Severance et al., 1995) described previously was used for these simulations. Again electrostatic decoupling (Bash et al., 1987) was employed and each free-energy calculation consisted of two consecutive simulations. In the first simulation, the partial charges on the radical were reduced to zero, whereas in the second simulation the bonds were shrunk to 0.3 Å while simultaneously reducing the Lennard-Jones parameter values to zero. Because flexible-molecule simulations tend to become unstable as the bond lengths become very small, the latter simulation was split into two stages. In the first stage the coupling parameter, λ, varied from 0 to an intermediate value, usually 0.5, while the equations of motion were integrated using a long time step of 2 fs and a short time step of 0.25 fs. In the second stage, λ varied from the intermediate value to 1, while the long and short times steps were set at 0.5 fs and 0.0625 fs, respectively.

Table 5 reports the ΔG_{solv} values from the flexible molecule simulations at four pressures in the range 275–2,100 bar at 773 K. The uncertainties for the single-run state points correspond to the difference between the forward and backward free-energy changes. The fugacity coefficients corresponding to the flexible-molecule simulations are shown as solid symbols in Figure 6. In the absence of experimental data it is not possible to make any judgment on whether the flexible or rigid models represent the HO_2-SCW system better. The data for both types of models show similar trends, although the flexible system exhibits an increase in the fugacity coefficient of HO_2 at lower values of pressure than does the rigid system.

Conclusions

This article demonstrates a method for calculating the fugacity coefficient of transient species such as free radicals in dense phases. The method involves application of fundamental principles including quantum mechanics to derive an appropriate force field for the solute (and if necessary, solvent) species and classical statistical mechanics to calculate the solvation free energy of the solute in the dense phase. As a test case we estimated the fugacity coefficient of the hydroperoxyl radical in supercritical water. The estimated values were much different from unity at the conditions studied and therefore

suggest that the ideal-gas approximation commonly used in kinetic modeling of reactions in supercritical water is not adequate. On the other hand, equation-of-state-based fugacity coefficients calculated using the critical properties from the thermodynamic database supplied with the Real Gas version of CHEMKIN (Schmitt et al., 1994) were in greater disagreement with our calculated values.

Acknowledgment

The Office of Vice-President for Research and the Horace H. Rackham School of Graduate Studies, University of Michigan, are gratefully acknowledged for partial support of this work through the Research Partnership Program.

Notation

K = equilibrium constant
N = number of molecules
P = pressure
R = gas constant or nuclear distance
T = absolute temperature
V = electrostatic potential
Z = compressibility factor or nuclear charge
k = rate constant
k_B = Boltzmann constant
q = charge
r = distance
s = electronic spin operator
ϵ = Lennard-Jones energy parameter
ϵ_0 = permitivity of free space
ν = stoichometric coefficient
σ = Lennard-Jones radius
θ = angle

Subscripts and superscripts

0 = reference value of property or standard state property
RW = radical-water property
W = water property
i = atomic index
j = atomic index
l = molecular index
m = molecular index
o = standard state property

Literature Cited

Allen, J., and D. Tildesley, *Computer Simulation of Liquids*, Oxford Univ. Press, Oxford (1987).

Andersen, H. C., "Rattle: A Velocity Version of the Shake Algorithm for Molecular Dynamics Calculations," *J. Comp. Phys.*, **52**, 24 (1983).

Balbuena, P. B., K. P. Johnston, and P. J. Rossky, "Molecular Dynamics Simulation of Electrolyte Solutions in Ambient and Supercritical Water: 1. Ion Solvation," *J. Phys. Chem.*, **100**, 2706 (1996).

Bash, P. A., U. C. Singh, R. Langridge, and P. A. Kollman, "Free Energy Calculations by Computer Simulations," *Science*, **236**, 564 (1987).

Ben-Naim, A., *Solvation Thermodynamics*, Plenum Press, New York (1987).

Berendsen, H. J. C., J. P. M. Potsma, W. F. van Gunsteren, and J. Hermans, "Interaction Models for Water in Relation to Protein Hydration," *Intermolecular Forces*, J. Jortner and B. Pullman, eds., Dordrecht, The Netherlands, p. 331 (1981).

Berendsen, H. J. C., J. P. M. Potsma, W. F. van Gunsteren, A. DiNola, and J. R. Haak, "Molecular Dynamics with Coupling to an External Bath," *J. Chem. Phys.*, **81**, 3684 (1984).

Boys, S. F., and F. Bernardi, "The Calculation of Small Molecular Interactions by the Differences of Separate Total Energies. Some Procedures with Reduced Errors," *Mol. Phys.*, **19**, 553 (1970).

Breneman, C. M., and K. B Wiberg, "Determining Atom-Centered Monopoles from Molecular Electrostatic Potentials. The Need for High Sampling Density in Formamide Conformational Analysis," *J. Comp. Chem.*, **11**, 361 (1990).

Brock, E. E., and P. E. Savage, "A Detailed Chemical Kinetics Model for the Supercritical Water Oxidation of C_1 Compounds," *AIChE J.*, **41**, 1874 (1995).

Brock, E. E., Y. Oshima, P. E. Savage, and J. R. Barker, "Kinetics and Mechanism of Methanol Oxidation in Supercritical Water," *J. Phys. Chem.*, **100**, 15834 (1996).

Cox, S. R., and D. E. Williams, "Representation of the Molecular Electrostatic Potential by Net Atomic Charge Model," *J. Comp. Chem.*, **2**, 304 (1981).

Frisch, M. J., M. Head-Gordon, G. W. Trucks, J. B. Foresman, H. B. Schlegel, K. Raghavachari, M. Robb, J. S. Binkley, C. Gonzalez, D. J. Defrees, D. J. Fox, R. A. Whiteside, R. Seeger, C. F. Melius, J. Baker, R. L. Martin, L. R. Kahn, J. J. P. Stewart, S. Topiol, and J. A. Pople, *GAUSSIAN90*, Rev. I. Gaussian, Pittsburgh (1990).

Gopalan, S., and P. E. Savage, "Phenol Oxidation in Supercritical Water," *Innovations in Supercritical Fluids: Science and Technology*, K. W. Hutchenson and N. R. Foster, eds., American Chemical Society, Washington, DC, ACS Symposium Series 608 p. 217 (1995).

Haile, J. M., "On the Use of Computer Simulation to Determine the Excess Free Energy in Fluid Mixtures," *Fluid Phase Equilibria*, **26**, 103 (1986).

Holgate, R. H., and J. W. Tester, "Fundamental Kinetics and Mechanisms of Hydrogen Oxygen in Supercritical Water," *Combust. Sci. Tech.*, **88**, 369 (1993).

Holgate, R. H., and J. W. Tester, "Oxidation of Hydrogen and Carbon Monoxide in Sub- and Supercritical Water: Reaction Kinetics, Pathways, and Water Density Effects 2. Elementary Reaction Modeling," *J. Phys. Chem.*, **98**, 810 (1994).

Hummer, G., and A. Szabo, "Calculation of Free Energy Difference from Computer Simulation of Initial and Final States," *J. Chem. Phys.*, **105**, 2004 (1996).

Jorgensen, W. L., J. Chandrasekhar, J. D. Madura, R. W. Impey, M. L. Klein, "Comparison of Simple Potential Functions for Simulation of Liquid Water," *J. Chem. Phys.*, **79** 926 (1983).

Jorgensen, W. L., and C. Ravimohan, "Monte Carlo Simulation of Differences in Free Energy of Hydration," *J. Chem. Phys.*, **83**, 3050 (1985).

Lazaridis, T., and M. E. Paulaitis, "Activity Coefficients in Dilute Aqueous Solutions from Free Energy Simulations," *AIChE J.*, **39**, 1051 (1993).

Liu, R., and N. L. Allinger, "Molecular Mechanics (MM3) Calculations on Alkyl Radicals," *J. Comp. Chem.*, **15**, 283 (1994).

Lubic, K. G., T. Amano, H. Uehara, K. Kawaguchi, and E. Hirota, "The ν_1 Band of the DO_2 Radical by Difference Frequency Laser and Diode Laser Spectroscopy: The Equilibrium Structure of the Hydroperoxyl Radical," *J. Chem. Phys.*, **81**, 4826 (1984).

Mizan, T. I., P. E. Savage, and R. M. Ziff, "Molecular Dynamics of Supercritical Water Using a Flexible SPC Model," *J. Phys. Chem.*, **98**, 13067 (1994).

Mizan, T. I., P. E. Savage, and R. M. Ziff, "A Molecular Dynamics Investigation of Hydrogen Bonding in Supercritical Water," *Innovations in Supercritical Fluids: Science and Technology*, K. W. Hutchenson and N. R. Foster, eds., American Chemical Society, Washington, DC, ACS Symposium Series 608, p. 47 (1995).

Mizan, T. I., P. E. Savage, and R. M. Ziff, "Temperature Dependence of Hydrogen Bonding in Supercritical Water," *J. Phys. Chem.*, **100**, 403 (1996a).

Mizan, T. I., P. E. Savage and R. M. Ziff, "Comparison of Rigid and Flexible Simple Point Charge Water Models at Supercritical Conditions," *J. Comp. Chem.*, **17**, 1757 (1996b).

Mizan, T. I., P. E. Savage, and R. M. Ziff, "Critical Point and Coexistence Curve for a Flexible Simple Point Charge Water Model," *J. Supercrit. Fluids*, in press (1997).

Møller, C., and M. S. Plesset, "Note on Approximation Treatment for Many-electron Systems," *Phys. Rev.*, **46**, 618 (1934).

Mulliken, R. S., "Electronic Population Analysis on LCAO-MO Molecular Wave Functions. I," *J. Chem. Phys.*, **23**, 1833 (1955).

Parkhill, S. M., "Pressure Cooking Toxic Wastes," *Compressed Air*, **4**, 16 (1995).

Parsons, E. J., "Organic Reactions in Very Hot Water," *CHEMTECH*, **26**, 30 (1996).

Pearlman, D. A., and P. A. Kollman, "A New Method for Carrying Out Free Energy Perturbation Calculations: Dynamically Modified Windows," *J. Chem. Phys.*, **90**, 2460 (1989).

Pople, J. A., M. Head-Gordon, D. J. Fox, K. Raghavachari, and L. A. Curtiss, "Gaussian-1 Theory: A General Procedure for Prediction of Molecular Energies," *J. Chem. Phys.*, **90**, 5622 (1989).

Reid, R. C., J. M. Prausnitz, and B. E. Pohling, *The Properties of Gases and Liquids*, McGraw-Hill, New York (1988).

Reynolds, C. A., P. M. King, and W. G. Richards, "Free Energy Calculations in Molecular Biophysics," *Mol. Phys.*, **76**, 251 (1992).

Saito, S., and C. Matsumura, "Dipole Moment of the HO_2 Radical from Its Microwave Spectrum," *J. Mol. Spectrosc.*, **80**, 34 (1980).

Sandler, S. I., *Chemical Engineering Thermodynamics*, 2nd ed., Wiley, New York (1989).

Savage, P. E., S. Gopalan, T. I. Mizan, C. J. Martino, and E. E. Brock, "Reactions at Supercritical Conditions: Applications and Fundamentals," *AIChE J.*, **41**, 1723 (1995).

Schoen, M., and C. Hoheisel, "The Mutual Diffusion Coefficient D_{12} in Binary Liquid Model Mixtures. Molecular Dynamics Calculations Based on Lennard-Jones (12-6) Potentials," *Mol. Phys.*, **52**, 33, (1984).

Schmitt, R. G., P. B. Butler, and N. Bergan French, *CHEMKIN Real Gas*, UIME PBB 93-006, Univ. of Iowa, Ames (1994).

Schmitt, R. G., and P. B. Butler, "Detonation Wave Structure of Gases at Elevated Initial Pressures," *Combust. Sci. Tech.*, **107**, 355 (1995).

Sealock, L. J., and D. C. Elliot, E. G. Barker, and R. S. Butner, "Chemical Processing in High-pressure Aqueous Environments. 1. Historical Perspective and Continuing Developments," *Ind. Eng. Chem. Res.*, **32**, 1535 (1993).

Severance, D. L., and W. L. Jorgensen, "Generalized Alteration of Structure and Parameters: A New Method for Free-energy Perturbations in Systems Containing Flexible Degrees of Freedom," *J. Comp. Chem.*, **16**, 311 (1995).

Shing, K. S., and S. T. Chung, "Computer Simulation Methods for the Calculation of Solubility in Supercritical Extraction," *J. Phys. Chem.*, **91**, 1674 (1987).

Siskin, M., and A. R. Katritzky, "Reactivity of Organic Compounds in Hot Water: Geochemical and Technological Implications," *Science*, **254**, 231 (1991).

Teleman, O., B. Jönsson, and S. Enström, "A Molecular Dynamics Simulation of a Water Model with Intramolecular Degrees of Freedom," *Mol. Phys.*, **60**, 193 (1987).

Tuckerman, M., B. J. Berne, and G. J. Martyna, "Reversible Multiple Time Scale Molecular Dynamics," *J. Chem. Phys.*, **97**, 1990 (1992).

Uehara, H., K. Kawaguchi, and E. Hirota, "Diode Laser Spectroscopy of the ν_2 and ν_3 Fundamental Bands of DO_2," *J. Chem. Phys.*, **83**, 5479 (1985).

Weiner, S. J., P. A. Kollman, D. T. Nguyen, and D. A. Case, "An All Atom Force Field for Simulations of Proteins and Nucleic Acids," *J. Comp. Chem.*, **7**, 230 (1986).

Zhu, S.-B., and C. F. Wong, "Sensitivity Analysis of Water Thermodynamics," *J. Chem. Phys.*, **98**, 8892 (1993).

Zwanzig, R. W., "High-temperature Equation of State by a Perturbation Method: I. Nonpolar Gases," *J. Chem. Phys.*, **22**, 1420 (1954).

Manuscript received Aug. 1, 1996, and revision received Dec. 16, 1996.